Proceedings of IMECE2005
2005 ASME International Mechanical Engineering Congress and Exposition
November 5-11, 2005, Orlando, Florida USA

IMECE2005-81801

LIFTING POSTURE ANALYSIS IN MATERIAL HANDLING USING VIRTUAL HUMANS

Joo H. Kim
Virtual Soldier Research (VSR) Program
Center for Computer-Aided Design
The University of Iowa

Karim Abdel-Malek
Virtual Soldier Research (VSR) Program
Center for Computer-Aided Design
The University of Iowa

Jingzhou Yang
Virtual Soldier Research Program
Center for Computer-Aided Design
The University of Iowa

Timothy Marler
Virtual Soldier Research Program
Center for Computer-Aided Design
The University of Iowa

Kyle Nebel
U.S. Army TACOM/RDECOM
AMSRD-TAR-NAC/157
Warren, MI

ABSTRACT

Adopting appropriate postures during manual material-handling tasks is the key to reducing human joint injuries. Although much experimentation has been conducted in an effort to model lifting, such an approach is not general enough to consider all potential scenarios in material handling. Thus, in this paper an optimization-based motion prediction method is used to simulate realistic lifting postures and predict joint torques to evaluate the risk level of injury.

A kinematically realistic digital human model has been developed such that the complicated musculoskeletal human structure is modeled as a combination of serial chains using the generalized coordinates. Lagrange's equations of motion and metabolic energy rate are derived for the digital human.

The proposed method has been implemented to predict and evaluate the lifting postures based on the metabolic rate and joint torques. Our results show that different amount of external loads and tasks lead to different human postures and joint torque distribution, thus different risk level of injury.

Keywords: lifting, posture, motion prediction, joint torque, Lagrangian, optimization

INTRODUCTION

Digital human models allow extensive analysis and simulation to be carried out in a virtual world rather than with an expensive mock-up. The users are able to get feedback from the simulation of certain tasks and performances of a human. For material handling, the simulation feedback is an important aspect of the task design procedure. The goal is to create methods and tools that allow for human analysis, design, and evaluation, without actually having a physical mock-up of the environment.

This paper addresses one such tool that will allow a user to predict human motion and performance level for a given task. To that end, we propose a general approach to mathematics-based dynamic motion prediction and analysis. We assume that a human naturally moves in such a way as to minimize certain cost functions. In the case of human behavior, we call the cost functions the human performance measures. Therefore, we propose the implementation of an optimization-based approach whereby human performance measures are developed and utilized to predict the realistic motion.

During manual lifting tasks, the lumbar spinal column (low-back) is the region where most back injuries occur as it is subjected to much greater loads than any other area of the spine (Gallagher *et al.* 2002). The reason for the high forces produced on the lower back during lifting activities is the vigorous contraction of back muscles to counteract the weight being lifted. Gallagher *et al.* have experimentally estimated the low-back muscle forces for four different cable-lifting postures (kneeling on one knee, kneeling on two knees, stooping, and standing) from the EMG data. The lumbar moments for each case were calculated from the muscle forces and muscle moment-arms. These were also compared with the cases for increased cable load. Chaffin (1997) has developed two- and three-dimensional computerized human models for simulation of static strength during work. This method can also predict some critical values of low-back, such as back compression loads and disc shear loads.

Considerable research has been done in postural analysis in material handling (Bobick 1987; Nussbaum and Torres 2001; Gallagher 1987; Gallagher *et al.* 2002; Chung and Kee 2000). Most of them used experiment-based methods.

On the other hand, there are several studies on human posture and motion simulation based on optimization. One of the most widely used cost functions in human simulation studies is the energy expenditure. Hase and Yamazaki (1997) have simulated walking and rowing motions using rigorous muscle energy expenditure formulas and human model. They have used the Newton-Euler method to calculate the joint torques. However, calculating the muscle energy expenditure directly from the element muscle fiber model requires tremendous computational efforts. Umberger *et al.* (2003) formulated rather simplified yet exact muscle energy expenditure, based on Hill-type muscle model and coefficients. Some simple examples, such as isolated muscle actions, single joint motion, and locomotion, were simulated and the computed energy values were compared with experimental results. Another approach for obtaining energy cost has been used by Alexander (1997). Alexander's energy formula is very simple and experiment-based. That energy cost was minimized to solve for realistic human arm trajectories.

The energy expenditure can also be related to fatigue prediction. Fatigue is a complex phenomenon, and it may be determined by several factors, including psychological health of the subjects. Although much is known about fatigue, its exact cause remains to be determined. At the biomechanical level, many literatures explain fatigue as loss of energy (Nicolson 2003). In the human gait motion, Anderson and Pandy (2001) suggested that minimizing muscle fatigue at each instant is roughly the same as minimizing metabolic energy expended per unit distance traveled over the duration of the gait cycle. In fact, it is well known that energy expenditure and muscle fatigue have positive correlation (Sahlin *et al.* 1998, Khang and Zajac 1989). Therefore, minimum metabolic energy expenditure indicates less muscle fatigue.

In this paper, we first present a modeling method for representing human upper body that can also be used for modeling any kinematic chain. Muscle models are also considered for dynamics formulation. We then derive general equations of motion and human energy expenditure formula in joint space. Using these equations, an optimization formulation is developed that allows for a computer program to simulate the natural human motions, joint torques and energy level. Then, some examples of motion/posture prediction for manual lifting tasks followed by joint torque evaluations are illustrated. By predicting the joint torques at the back and shoulder, the risk level of injury can be evaluated. Conclusions and future work are addressed.

KINEMATIC HUMAN MODELING AND GENERALIZED COORDINATES

To describe the human postures and motions, we use a kinematic pair as used in the study of robotics. A digital human model called Santos™, developed by The University of Iowa, has more than 100 degree-of-freedom (DOF), where all the joints are modeled as revolute joints. The shoulder joint, for example, has three degrees of freedom and is usually modeled as a spherical joint in the literatures. In our model, we combine three revolute joints at one location to represent the three degrees-of-freedom spherical shoulder joint. For upper body motion prediction, we use a 21 DOF Santos™ model from the waist to the right hand as shown in Figure 1. Here, joint 1 corresponds to lateral bending of low-back, joint 2 corresponds to flexion/extension of low-back, and so on.

Figure 1. 21 Degrees-of-freedom Santos™ model

The position vector of a point of interest on the end-effector of a human articulated model can be written in terms of joint coordinates as

$$\mathbf{x} = \mathbf{x}(\mathbf{q}) \tag{1}$$

where $\mathbf{q} = [q_1 \quad \dots \quad q_n]^T \in \mathbf{R}^n$ is the vector of *n*-generalized joint coordinates defining the motion of a link with respect to another. The global position vector $\mathbf{x}(\mathbf{q})$ can be obtained from the multiplication of the 4x4 homogeneous transformation matrices ${}^{i-1}\mathbf{T}_i$, defined by the Denavit-Hartenberg (D-H) representation method (Denavit and Hartenberg, 1955).

$${}^{i-1}\mathbf{T}_i(q_i) = \begin{bmatrix} \cos q_i & -\cos\alpha_i \sin q_i & \sin\alpha_i \sin q_i & a_i \cos q_i \\ \sin q_i & \cos\alpha_i \cos q_i & -\sin\alpha_i \cos q_i & a_i \sin q_i \\ 0 & \sin\alpha_i & \cos\alpha_i & d_i \\ 0 & 0 & 0 & 1 \end{bmatrix} \tag{2}$$

where q_i is the joint angle from $\mathbf{x}_{i-1}$ axis to the $\mathbf{x}_i$ axis for a revolute joint, d_i is the shortest distance between $\mathbf{x}_{i-1}$ and $\mathbf{x}_i$ axes, a_i is the offset distance between $\mathbf{z}_i$ and $\mathbf{z}_{i-1}$ axes, and α_i is the offset angle from $\mathbf{z}_{i-1}$ and $\mathbf{z}_i$ axes. Then the 4x4 transformation matrix ${}^0\mathbf{T}_i$ used to represent i^{th} joint coordinate system with respect to the global base coordinate system (0^{th}) is

$${}^0\mathbf{T}_i(\mathbf{q}) = {}^0\mathbf{T}_1(q_1)\,{}^1\mathbf{T}_2(q_2)\ldots{}^{i-1}\mathbf{T}_i(q_i) \tag{3}$$

We use the augmented 4x1 vector ${}^0\mathbf{r}_i$ and ${}^i\mathbf{r}_i$ to express the Cartesian coordinate of the point fixed in the i^{th} local frame in terms of global and local coordinate system, respectively:

$${}^0\mathbf{r}_i = \begin{bmatrix} \mathbf{x}(\mathbf{q}) \\ 1 \end{bmatrix}, \quad {}^i\mathbf{r}_i = \begin{bmatrix} {}^i\mathbf{x} \\ 1 \end{bmatrix} \tag{4}$$

where ${}^i\mathbf{x}$ is the fixed point at the link *i* and expressed with respect to the i^{th} coordinate system. Using these relationships, ${}^0\mathbf{r}_i$ can be written as

$${}^0\mathbf{r}_i = {}^0\mathbf{T}_i(q_1,\ldots,q_i)\,{}^i\mathbf{r}_i \tag{5}$$

MUSCLE MODEL AND JOINT STIFFNESS

A muscle is perceived as an actuator input into the musculoskeletal system where each joint is powered by one or more such actuators. In other words, muscle-generated forces empower and control all human movements and postures. The muscle-tendon systems have certain elastic properties that generate restoring forces at the joint. These restoring forces need to be included in the force equilibrium of muscle-link system.

Several muscle models were proposed in the literature, perhaps most notably the Hill's model (Hill, 1938) and the Zajac Muscle model (Zajac, 1989), which is a modified Hill's model. Most of the proposed muscle models have two main components: contractile components and series/parallel elastic components (Figure 2).

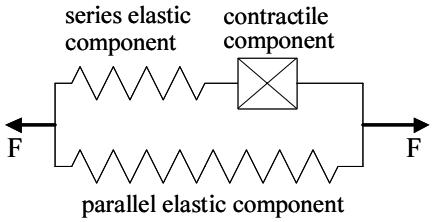

Figure 2. A typical Muscle Model

The muscle contractile elements generate tension force by contracting, and act as actuators. The elastic elements of muscles generate restoring forces in the corresponding independent degree-of-freedom for each joint motion (where each joint may have many muscle degrees of freedom). These effects are often complex in nature due to the variable and nonlinear muscle configurations during movement. Considering only the effective elastic behavior at the joint, we can regard the whole muscle elasticity mapped to the joint space as a nonlinear rotational spring attached to, and "felt" by each joint. Indeed, there exists a resultant rotational joint stiffness at each joint, which has the same effect as actual muscle elasticity. Therefore, any change of the joint angle from neutral position will result in a restoring torque $\tau_i^{\text{Restoring}}$, which can be linearly approximated as:

$$\tau_i^{\text{Restoring}} \approx -k_i \left(q_i - q_i^N \right) \ , \ i = 1,...,n \tag{6}$$

where k_i is appropriate equivalent rotational joint stiffness for each generalized joint spring, and q_i^N is the neutral joint variable corresponding to i^{th} joint angle q_i. The neutral joint variable is the natural unstretched joint configuration where the moment about a joint due to all the corresponding muscle forces are balanced without any external load or joint actuator torque. The coefficient k_i for each q_i is obtained from the simulation experiments based on the muscle physiological cross sectional area (PCSA). In vector-matrix form, this equation is rewritten as below.

$$\boldsymbol{\tau}^{\text{Restoring}} = -\mathbf{K}\left(\mathbf{q} - \mathbf{q}^N\right) \tag{7}$$

where $\mathbf{q}^N$ is the vector of neutral joint angle, and $\mathbf{K}$ is a diagonal matrix of joint stiffness.

LAGRANGE'S EQUATIONS OF MOTION

A general Lagrange's equation in vector-matrix form is

$$\frac{d}{dt}\frac{\partial (W+T)}{\partial \dot{\mathbf{q}}} - \frac{\partial (W+T)}{\partial \mathbf{q}} = \mathbf{0} \tag{8}$$

where $\mathbf{q}$ is the generalized coordinate vector, T is the total kinetic energy of the system, W is the virtual work done by (non-inertial) forces and torques. The virtual work is the sum of the virtual works done by conservative forces and non-conservative forces, i.e., $W = W_c + W_{nc}$. The conservative work can be expressed as the negative of the potential energy of the force system, i.e., $\delta W_c = -\delta V$. Thus we can write

$$\delta (W+T) = \delta T - \delta V + \delta W_{nc} = \delta L + \delta W_{nc} \tag{9}$$

where V is the total potential energy of the system, W_{nc} is the virtual work done by non-conservative forces and torques, and $L = T - V$ is called the Lagrangian function. Then equation (8) can be written as follows.

$$\frac{d}{dt}\frac{\partial L}{\partial \dot{\mathbf{q}}} - \frac{\partial L}{\partial \mathbf{q}} - \frac{d}{dt}\frac{\partial W_{nc}}{\partial \dot{\mathbf{q}}} - \frac{\partial W_{nc}}{\partial \mathbf{q}} = \mathbf{0} \tag{10}$$

We will derive more explicit form of the equation for a general serial manipulator and force system shown in Figure 3.

The velocity of a point fixed in the i^{th} local frame with differential mass dm in link i can be expressed in terms of global coordinate system as follows.

$$\mathbf{v}_i = \frac{d}{dt}\left({}^0\mathbf{r}_i\right) = \frac{d}{dt}\left({}^0\mathbf{T}_i\, {}^i\mathbf{r}_i\right) = \left(\sum_{j=1}^{i} \frac{\partial\, {}^0\mathbf{T}_i(\mathbf{q})}{\partial q_j} \dot{q}_j \right) {}^i\mathbf{r}_i \tag{11}$$

Then the total kinetic energy K of the human link system is

$$K = \sum_{i=1}^{n} K_i = \frac{1}{2} \sum_{i=1}^{n} \int_m Tr(\mathbf{v}_i \mathbf{v}_i^T)\, dm \tag{12}$$

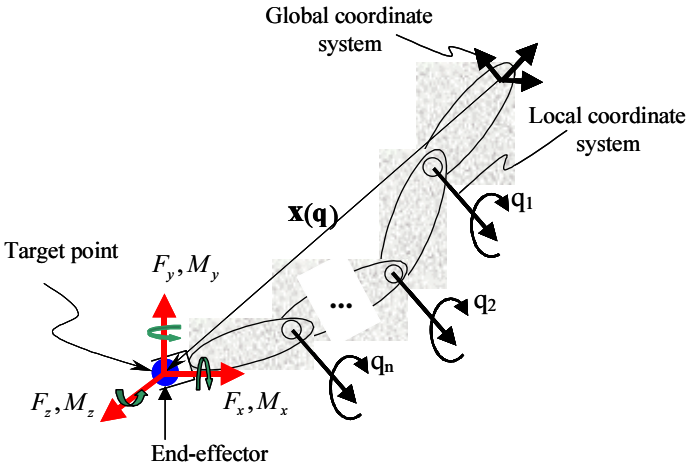

Figure 3. Joint-link system with external loads

The total potential energy P due to gravity is the sum of each link's potential energy.

$$P = \sum_{i=1}^{n} P_i = \sum_{i=1}^{n} -m_i \mathbf{g}^T ({}^0\mathbf{T}_i \, {}^i\bar{\mathbf{r}}_i) \tag{13}$$

where ${}^i\bar{\mathbf{r}}_i$ is the center of mass vector of link i with respect to the i^{th} local coordinate frame and $\mathbf{g}$ is the augmented (4x1) gravity vector.

Next, we assume that the applied non-conservative forces are actuating torques at the joints and external loads at the end-effector. Then the variation of virtual work done by non-conservative forces is

$$\delta W_{nc} = \delta\mathbf{q}\bullet\boldsymbol{\tau} + \delta\mathbf{x}\bullet\mathbf{F} + \delta\boldsymbol{\theta}\bullet\mathbf{M} = \delta\mathbf{q}^T\boldsymbol{\tau} + \begin{bmatrix}\delta\mathbf{x}\\ \delta\boldsymbol{\theta}\end{bmatrix}^T \begin{bmatrix}\mathbf{F}\\ \mathbf{M}\end{bmatrix} \tag{14}$$

where $\boldsymbol{\tau} = [\tau_1, \tau_2, ..., \tau_n]^T$ is the joint torque vector (actuated by muscles), $\mathbf{x}$ is the (3×1) Cartesian coordinate of the point of application of external force $\mathbf{F}$ (a 3×1 vector), and $\boldsymbol{\theta}$ is the (3×1) orientation vector of the link with respect to the global frame, where the external moment $\mathbf{M}$ (a 3×1 vector) is applied. Assuming that the velocity-dependent forces doesn't exists i.e., $d(\partial W_{nc}/\partial\dot{\mathbf{q}})/dt = 0$, the last term of equation (10) can be expanded as

$$-\frac{\partial W_{nc}}{\partial \mathbf{q}} = -\boldsymbol{\tau} - \frac{\partial}{\partial \mathbf{q}}\begin{bmatrix}\mathbf{x}\\ \boldsymbol{\theta}\end{bmatrix}^T \begin{bmatrix}\mathbf{F}\\ \mathbf{M}\end{bmatrix} = -\boldsymbol{\tau} - \mathbf{J}^T \begin{bmatrix}\mathbf{F}\\ \mathbf{M}\end{bmatrix} \tag{15}$$

where $\mathbf{J}$ is the Jacobian matrix (Sciavicco and Siciliano 1996). The above derivation can easily extended to the case where multiple external loads are applied to any location of any link, not necessarily to the end-effector. Likewise, the restoring torque $\boldsymbol{\tau}^{\text{Restoring}}$ introduced earlier can also be included in the above equation in the similar manner.

Based on the procedures given in Fu *et al.* (1987) with some modifications, equation (10) can be expanded using the kinetic energy (12), the potential energy (13), and the extended form of non-conservative work (15). Thus the final vector-matrix form of the equations of motion for human joint-link system with several external loads is shown below as coupled, nonlinear, second-order ordinary differential equations.

$$\boldsymbol{\tau} = \mathbf{M}(\mathbf{q})\ddot{\mathbf{q}} + \mathbf{V}(\mathbf{q},\dot{\mathbf{q}}) + \sum_i \mathbf{J}_i^T m_i \mathbf{g} + \sum_k \mathbf{J}_k^T \begin{bmatrix}-\mathbf{F}_k\\ -\mathbf{M}_k\end{bmatrix} + \mathbf{K}\left(\mathbf{q} - \mathbf{q}^N\right) \tag{16}$$

where $\mathbf{M}(\mathbf{q})$ is the mass-inertia symmetric matrix, $\mathbf{V}(\mathbf{q},\dot{\mathbf{q}})$ is the Coriolis and Centrifugal vector, $\sum \mathbf{J}_i^T m_i \mathbf{g}$ is the joint torque vector due to gravity force, $\mathbf{J}_i$ is the Jacobian matrix of the position vector for the center of mass of the i^{th} link, and $\mathbf{J}_k$ is the Jacobian matrix (for any point in any local coordinate) of the point at ${}^k r_k$ (4×1) location vector with respect to k^{th} local coordinate frame:

$$\mathbf{J}_k(\mathbf{q}) = \begin{bmatrix} \frac{\partial {}^0\mathbf{T}_k(\mathbf{q})}{\partial q_1} {}^k\mathbf{r}_k & \cdots & \frac{\partial {}^0\mathbf{T}_k(\mathbf{q})}{\partial q_i} {}^k\mathbf{r}_k & \cdots & \frac{\partial {}^0\mathbf{T}_k(\mathbf{q})}{\partial q_k} {}^k\mathbf{r}_k \\ \mathbf{Z}_0(\mathbf{q}) & \cdots & \mathbf{Z}_{i-1}(\mathbf{q}) & \cdots & \mathbf{Z}_{k-1}(\mathbf{q}) \end{bmatrix}_{6\times k} \tag{17}$$

where $\mathbf{Z}_{i-1}$, $i = 1,...,k$ is the local z-axis vector of joint i expressed in terms of the global coordinate system. Here, we only take the first three elements of the (4×1) vectors $(\partial {}^0\mathbf{T}_k(\mathbf{q})/\partial q_i)\,{}^k\mathbf{r}_k$.

To apply the above equations of motion to the human joint-link system, some physical characteristics of anatomical segments are needed to determine the coefficients in the equations of motion. These physical properties are: mass of each link, center of mass for each link, moments of inertia for each link, and joint stiffness.

Our digital human, Santos™, is modeled based on a typical male soldier anthropometry data. For simplicity, all the links of Santos™ are modeled as thin rods, so that the moments of inertia are calculated easily using the link lengths and radii of gyration. The mass and center of mass data are obtained from Chaffin *et al.* (1999) and Mi (2004), and then modified to fit into our Santos™ model. The joint stiffness is estimated from the stiffness of all the muscles involved in each degree-of-freedom joint movement.

HUMAN ENERGY EXPENDITURE RATE

Skeletal muscles may be thought of as the biochemical machines with chemical energy stored in ATP going into the muscles converted to mechanical work and heat energy (Sherwood 1997, Umberger, *et al*. 2002). In other words, the total metabolic energy expenditure will be transformed mainly into the sum of work done by the joint torques, heat energy dissipation, and basal metabolic energy. In the case of static loading, where the mechanical work done by muscle is zero, the muscle energy is all dissipated as heat.

The mechanical power is defined as the product of joint torque and joint velocity. The total mechanical power of the system $\dot{W}$ is the sum of the mechanical power for all the joints.

$$\dot{W} = \sum_{i=1}^{n} \left|\dot{W}_i\right| = \sum_{i=1}^{n} \left|\tau_i \dot{q}_i\right| \tag{18}$$

Note that, since the torque τ_i and the joint velocity $\dot{q}_i$ are functions of time, the total mechanical power $\dot{W}$ is also a function of time. In other words, the values of mechanical power can be evaluated at each time instant. The absolute values in equation (18) mean that the mechanical energy consumed by the muscle cannot be reduced by simultaneous production of negative power by another muscle at the same time, or by the same muscle during different periods of time.

Based on several heat energy formula for longitudinal muscle model (Hase and Yamazaki 1997, Khang and Zajac 1989), the muscle heat expenditure is divided into two components: (i) Muscle maintenance heat and (ii) muscle shortening heat. The muscle maintenance heat is the energy consumed in proportion to the muscular tension. The muscle

shortening heat is the energy consumed in proportion to muscle shortening rate. It is necessary to convert these relations in muscle space into the generalized coordinate system, i.e., the joint space, by using the heat energy equation given in Hase and Yamazaki (1997).

For a given muscle, the muscle maintenance heat rate is calculated as the product of a constant and muscle activation. From the studies on muscle activation (Anderson and Pandy 2001), we observe that the generalized maintenance heat rate is approximately proportional to the joint torque and inversely proportional to the maximum torque limit. So, in terms of joint space, the generalized maintenance heat rate $\dot{Q}_m$ is

$$\dot{Q}_m \approx \sum_{i=1}^{n} h_m^i |\tau_i| \tag{19}$$

where $h_m^i \quad (i = 1,...,n)$ is the generalized coefficient of the maintenance heat at joint *i*. These coefficients are assigned to each joint, and are obtained from the maximum voluntary torque data.

The amount of muscle shortening heat is usually small compared to that of the maintenance heat (Bhargava, *et al*. 2004, Anderson and Pandy 2001). For this reason and for further simplicity, we neglect the contribution of muscle shortening heat. Furthermore, this term resembles the form of muscle mechanical power. So, by adjusting the coefficients $h_m^i \quad (i = 1,...,n)$ of the generalized maintenance heat $\dot{Q}_m$, we can obtain good approximation of total muscle energy rate.

The basal metabolic rate, BMR is defined as the rate at which heat is produced by an individual in a resting state. BMR indicates the minimum amount of energy needed to carry out metabolism or visceral activity at rest. We use the formula used by Hase and Yamazaki (1997) for estimation of BMR. The BMR of the whole body is estimated as follows.

$$\dot{B} = 0.685W + 29.8 \quad \text{(Joule/second or Watt)} \tag{20}$$

where W (Kg) is the body mass.

Finally, the human metabolic energy expenditure rate is the sum of mechanical power, heat rate, and BMR.

$$\dot{E}_{Metabolic} \approx \sum_{i=1}^{n} |\tau_i(t)\dot{q}_i(t)| + \sum_{i=1}^{n} h_m^i |\tau_i(t)| + \dot{B} \tag{21}$$

OPTIMIZATION AND MOTION/POSTURE PREDICTION

We use an optimization-based technique for motion prediction. This is based on our assumption that human moves in such a way to minimize certain human performance measures, subject to some physical and physiological constraints. Several human performance measures have been investigated and shown to produce various natural motions and postures (Yang *et al*. 2004, Kim *et al*. 2004). In this paper, the metabolic energy expenditure, as described in the previous section, is used as a human performance measure for general motion prediction.

For motion prediction, we use the B-Spline method, which is widely used for manipulator motion studies. Therefore, the joint angles, joint velocities, and joint accelerations are all linear functions of the control points of the B-Spline curves. The optimization procedure calculates the joint angle profiles of every joint in the form of B-Spline curves for natural upper-body motion. Also, the joint velocity and acceleration profiles are directly obtained in terms of control points from the direct calculation of the B-Spline. The optimization problem for motion prediction can be stated as follows:

Find: Control Points ($P_{i,j} \quad i = 1,...,m;\ j = 1,...,n$)

To minimize: Metabolic Energy ($E_{Metabolic}$)

Subject to:

- Joint limits ($q_i^L \le q_i \le q_i^U \quad i = 1,...,n$)
- Torque limits ($\tau_i^L \le \tau_i \le \tau_i^U \quad i = 1,...,n$)
- Path constraints ($\| \mathbf{x}(\mathbf{q}(t)) - \mathbf{p}(t) \| \le \varepsilon$)
- Equations of motion

$$\boldsymbol{\tau} = \mathbf{M}(\mathbf{q})\ddot{\mathbf{q}} + \mathbf{V}(\mathbf{q},\dot{\mathbf{q}}) + \sum \mathbf{J}_i^{\mathrm{T}} m_i \mathbf{g} + \sum \mathbf{J}_k^{\mathrm{T}} \mathbf{F}_k + \mathbf{K}\left(\mathbf{q} - \mathbf{q}^N\right)$$

When the optimization is performed at each time interval, the resulting joint kinematic profiles are used as inputs for the equations of motion. This will then solve the inverse dynamics problem for the required joint torques. The energy expenditure rate at each time instant is also calculated throughout the motion.

In our study, we use SNOPT software package developed by Gill *et al.* (2002). The SNOPT package is a general-purpose system for solving optimization problems involving many variables and constraints, based on a sequential quadratic programming (SQP) method.

EXAMPLE RESULTS AND ANALYSIS

In this section, some examples of lifting-motion prediction and joint torque evaluation are considered for the 21-DOF Santos™ upper-body model.

Example 1. Prediction and analysis of dynamic pulling motions

The task is to predict the motion of pulling a rope with constant tension from a given initial position, to a given final position in 2 seconds. The rope is stretched horizontally toward the right side of a human where a counter-weight is hanging at the other end of the rope around a pulley. Figures 4 and 8 show the resulting predicted motions. For motion 1A (Figure 4), a 0.001 Kg. counter-weight is hanging at the other end of the rope.

The resulting optimum joint kinematic profiles are obtained at each 0.04 seconds and are shown in Figure 5. At each time, the joint torque values and the metabolic energy rate are calculated (Figures 6 and 7). The metabolic energy expended for this motion is 234.89 (Joules).

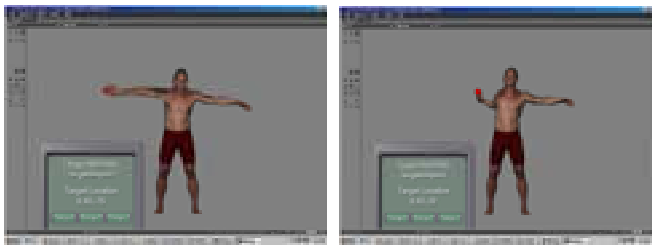

(a) t = 0 second (initial) (b) t = 2 seconds (final)

Figure 4. Predicted motion of Example 1A: Pulling a rope with 0.001 Kg. load

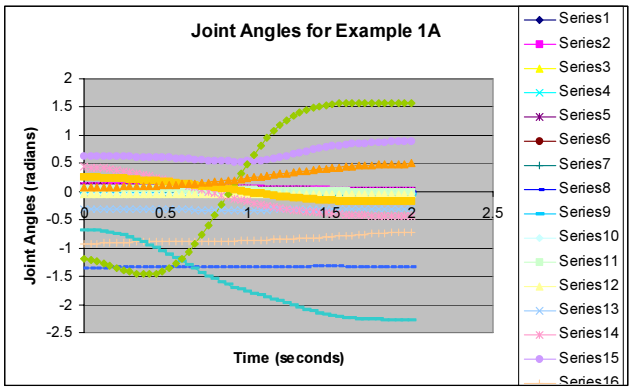

Figure 5. Predicted joint profiles for motion Example 1A

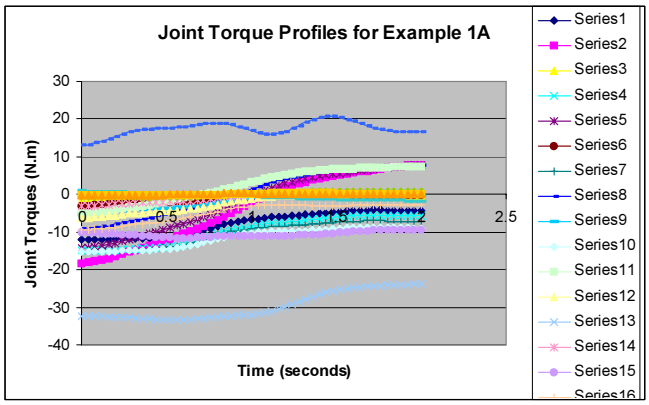

Figure 6. Predicted joint torques for Example 1A

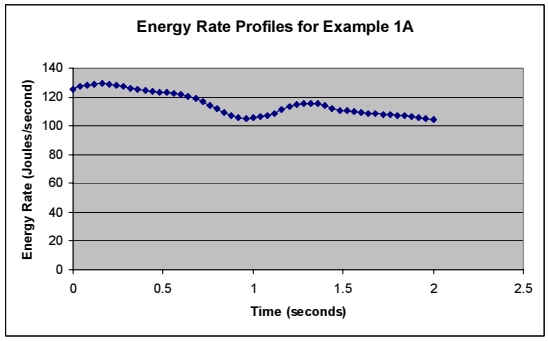

Figure 7. Predicted energy rate profile for motion Example 1A

For motion 1B (Figure 8), a 27 Kg counter-weight is hanging at the other end of the rope. This task is same as 1A, except for the amount of counter-weight (0.001 Kg vs. 27 Kg). It is observed that Santos™ generated different motions for different amount of external loads required. For larger tension (27 Kg. weight, in this case), Santos™ tilted his trunk to use his own body weight. In this way digital human could also straighten his right arm to minimize the joint torques at the wrist and elbow.

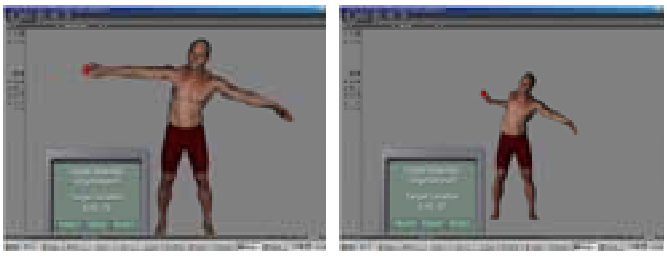

(a) t = 0 second (initial) (b) t = 2 seconds (final)

Figure 8. Predicted motion of Example 1B: Pulling a rope with 27 Kg. load

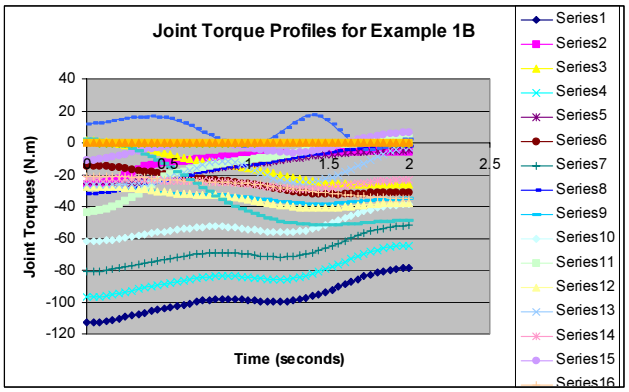

Figure 9. Predicted joint torques for Example 1B

In Figure 9, the high negative torque values at joints 1, 4, 7, and 10 for motion 1B indicate the major contributions of these joints to the left lateral bending motion. These large torques are used to move the body while balancing with the large external pulling force.

The metabolic energy consumed during this motion is 614.24 (Joules). As expected, this value is much higher than the energy expenditure of pulling with 0.01 N (234.89 (Joules)).

Example 2. Lifting same weight at different locations

In this and the following examples, we consider the initial posture of each motion to predict the risk level of injury at the onset of the task.

Figures 10 and 11 show two different onset postures of manual lifting tasks. In posture 2A, a 9 kg object on hand is located far right from the body and in posture 2B, the same weight is located far front from the body.

With the velocities and accelerations set to zero (static onset posture), the equations of motion (16) are used to obtain the torque at each joint. The joint torques of both postures are plotted in Figure 12.

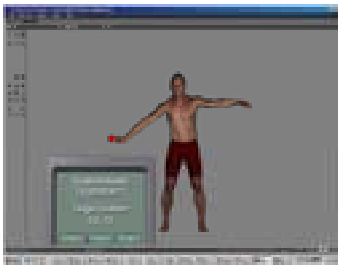

Figure 10. Posture 2A

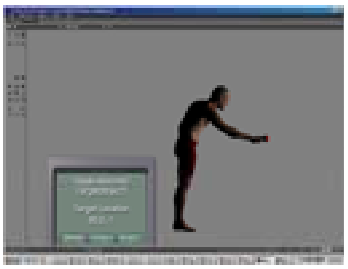

Figure 11. Posture 2B

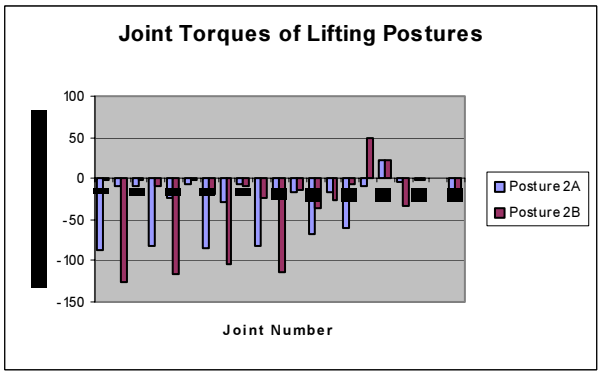

Figure 12. Joint torques of lifting postures 2A and 2B

In posture 2A, the spine joints for lateral bending exert large torques for right lateral bending, while in posture 2B, the spine joints for flexion/extension exert large torques for flexion. The large torque values for different motion segments will have different effects on the body and may cause different kind and risk level of injury (especially on the low-back). It can be observed that the two postures have different torque distributions at the shoulder and arm joints.

Using equation (21), the energy expenditure rate is calculated as 275.5 (Joules/sec) for posture 2A and 308.3 (Joules/sec) for posture 2B. These values are within reasonable range of energy expenditure rate during weight lifting exercise (Sherwood 1997).

Example 3. Lifting same weight with different postures

A manual task of lifting a 10-Kg object with two different postures is studied in this example. The two predicted postures are shown in Figures 13 and 14. In each case, Santos™ is holding the object so that the palm faces upward. Posture 3A is the lifting posture where the right arm is stretched forward and the object is far from the body, located at (-30, 20, 65) (cm) with respect to the global frame at the lumbar region (Figure 1). In posture 3B, the right elbow is bent and the object is brought closer to the body, i.e., (-30, 15, 40) (cm) from the global frame. The resulting joint torques for both postures are plotted in Figure 15.

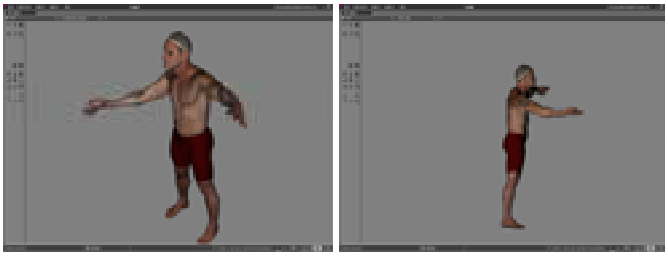

(a) Oblique view (b) Side view

Figure 13. Posture 3A

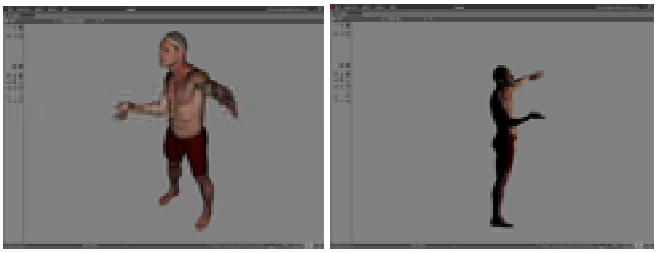

(a) Oblique view (b) Side view

Figure 14. Posture 3B

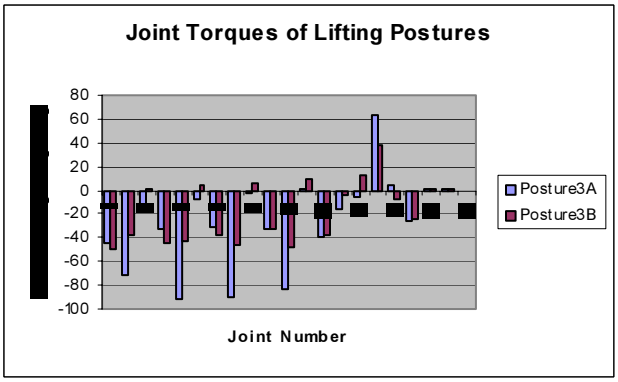

Figure 15. Joint torques of lifting postures 3A and 3B

As indicated in Figure 15, holding the object far from the body requires the muscles of the low back to exert an extension torque of 71.7 (N.m) at joint 2 (flexion/extension joint of low-back). However, if the weight is located closer to the body, only 37.7 (N.m) torque is required at joint 2. The similar change can be observed at other joints that exert extension torques, i.e., joints 5, 8, and 11. The reduced joint torque exerted by the back muscles will diminish the load experienced by the spine and therefore will reduce the risk of back injury.

The big difference in torque values can be found also in joints 14 and 16. These are abduction/adduction of the clavicle and shoulder joint, respectively. Just as the low back joint case, this is due to the difference in the lever-arm length. Thus, posture 3A is more likely to generate muscle fatigue than posture 3B. This gives another reason that the load should be kept close to the body during manual lifting.

Holding an object at a far distance from the body requires a large amount of torques to be exerted by the back and shoulder muscles while the amount of torques can be reduced by holding the object closer to the body. Thus, our result supports the recommendation that workers should keep the load close during manual lifting tasks to prevent injury.

The energy expenditure rate for posture 3A is calculated as 288.3 (Joules/sec), while for posture 3B, it is 230.4 (Joules/sec). It can be seen that the value of energy expenditure rate for any time instant gives us a single criteria that evaluates the level of "effort" of a given posture.

CONCLUSIONS AND DISCUSSION

An optimization-based method and examples of motion/posture prediction and analysis for manual lifting were introduced. The results have shown that our model, formulation, and method can be extended to analyze any kind of general material handling. Our method for motion prediction and analysis can be very helpful in determining the risk of injury during manual lifting tasks. The evaluation of joint torques during lifting can help the user to redesign tasks so that the stresses on the low-back and shoulder are decreased. The simulation also showed how Santos^{TM} generates different motions and postures in response to different amount of external loads.

A general form of dynamic equations of motion were derived and used to obtain the metabolic energy expenditure formula. It is also used to solve the inverse dynamics problem of the motion prediction. This equations of motion include the general external loads (forces and moments) applied not only to the end-effector (hand), but also to any other parts of the body. This generalization of point of force-application enables us to simulate the cases when a human is hanging a bag on the forearm, wearing a backpack on the shoulder, and so forth. The metabolic energy expenditure was used as a cost function to be minimized. By rearranging the metabolic energy rate formula, it is observed that the energy rate is a summation of weighted joint torques, where the weight function is the sum of the corresponding joint velocity and the heat coefficient. This minimum energy cost criteria implicitly indicates minimum joint torques and thus, the motion based on minimum energy is equivalent to the motion of minimum joint torques.

The joint torque solutions of the inverse dynamics can be used as an input for the prediction of muscle force distribution. For the purpose of motion/posture prediction, the principle of generalized coordinates and generalized torques provided us with a simplified and accurate kinematical model. However, multiple muscles contribute to a single degree-of-freedom joint motion and the actual configuration of muscles varies as the corresponding joint moves. This leads us to the future studies of detailed biomechanical analysis on muscle forces and deformations, and then to muscle fatigue prediction. Finally, to obtain more accurate value for the energy expenditure and joint torques, we will acquire more exact data of physical properties, such as centers of masses, moments of inertia, and products of inertia.

Although our simulation results are kinematically realistic, the actual human body is more complex and flexible than the Santos^{TM} model. Especially for the detailed study of the spine, a higher degrees-of-freedom model should be used to improve accuracy. Our future work is to incorporate muscles to build higher degrees-of-freedom model that is anatomically realistic. This will also enable us to investigate the muscle forces and fatigue properties during material handling task.

ACKNOWLEDGMENTS

This research is funded by the US Army TACOM project: Digital Humans and Virtual Reality for Future Combat Systems (FCS).

REFERENCES

1. Alexander, R.M., 1997, "A minimum energy cost hypothesis for human arm trajectories", *Biological Cybernetics*, n 76 1997, p 97-105.
2. Anderson, F.C., Pandy, M.G., 2001, "Static and dynamic optimization solutions for gait are practically equivalent", *Journal of Biomechanics*, v 34, Issue 2, February 2001, p 153-161.
3. Bhargava, L.J., Pandy, M.G., Anderson, F.C., 2004, "A phenomenological model for estimating metabolic energy consumption in muscle contraction", *Journal of Biomechanics*, v 37, n 1, January, 2004, p 81-88.
4. Bobick, T.G., 1987, "Analysis of material-handling systems in underground low-coal mines", *Information Circular - United States, Bureau of Mines*, 1987, p 13-20.
5. Chaffin, D.B., 1997, "Development of computerized human static strength simulation model for job design", Human Factors and Ergonomics in Manufacturing, v 7 1997, p 305-322.
6. Chaffin, D.B., Andersson, G.B.J., Martin, B.J., 1999, *Occupational Biomechanics*, 3rd Edition, J. Wiley & Sons, New York, NY 1999.
7. Chung, M.K., and Kee, D., 2000, "Evaluation of lifting tasks frequently performed during fire brick manufacturing processes using NIOSH lifting equations", *International Journal of Industrial Ergonomics*, v 25, n 4, Apr, 2000, p 423-433.
8. Fu, K.S., Gonzalez, R.C., Lee, C.S.G., 1987, *Robotics: Control, Sensing, Vision, and Intelligence*, McGraw-Hill, 1987.
9. Gallagher, S., 1987, "Back strength and lifting capacity of underground miners", *Information Circular - United States, Bureau of Mines*, 1987, p 21-32.
10. Gallagher, S., Marras, W.S., Davis, K.G., Kovacs, K., 2002, "Effects of posture on dynamic back loading during a cable lifting task", *Ergonomics*, v 45, n 5, 2002, p 380-398.
11. Gill, P.E., Murray, W., Saunders, M. A., 2002, "SNOPT: An SQP algorithm for large-scale constrained optimization", *SIAM J. Optim.*, 12 (2002), pp. 979–1006.

12. Hase, K., Yamazaki, N., 1997, “Development of three-dimensional whole-body musculoskeletal model for various motion analyses”, *JSME International Journal*, Series C, v 40 n 1 Mar 1997, p 25-32.
13. Hill, A.V., 1938, “The heat of shortening and the dynamic constants of muscle”, *Proc. R. Soc. Lond.*, v 126, p 136-195.
14. Khang, G., Zajac, F.E., 1989, “Paraplegic standing controlled by functional neuromuscular stimulation - I: Computer model and control-system design”, *IEEE Transactions on Biomedical Engineering*, v 36, n 9, p 873-884.
15. Kim J., Abdel-malek, K., Mi, Z., and Nebel, K., 2004, “Layout Design Using an Optimization-based Human Energy Consumption Formulation”, *SAE Digital Human Modeling for Design and Engineering*, June 15-17, 2004, Rochester, Michigan, USA.
16. Nussbaum, MA, and Torres, N., 2001, “Effects of training in modifying working methods during common patient-handling activities”, *International Journal of Industrial Ergonomics*, v 27, n 1, Jan, 2001, p 33-41.
17. Sciavicco, L. and Siciliano, B., 1996, *Modeling and Control of Robot Manipulators*, McGraw Hill.
18. Sherwood, L., 1997, *Human Physiology: from cells to systems*, Third edition, Chapter 8 and Chapter 17, Wadsworth Publishing Co.
19. Umberger, B.R., Gerritsen, K.G.M., Martin, P.E., 2003, “A model of human muscle energy expenditure”, *Computer methods in biomechanics and biomedical engineering*, v 6, n 2, 2003, p 99-111.
20. Yang, J., Marler, R.T., Kim, H., Arora, J., and Abdel-Malek, K., 2004, “Multi-objective Optimization for Upper Body Posture Prediction”, *10th AIAA/ISSMO Multidisciplinary Analysis and Optimization Conference*, August, Albany, NY.